Int. J. Heat Mass Transfer. Vol. 36, No. 17, pp. 4247–4256, 1993
Printed in Great Britain

0017–9310/93 $6.00+0.00

Turbulent buoyant flows into a two dimensional storage tank

L. CAI and W. E. STEWART, JR.
Energy Research Laboratory, University of Missouri–Kansas City, Truman Campus, Independence, MO 64050-1799, U.S.A.

and

C. W. SOHN
U.S. Army Corps of Engineers, Construction Engineering Research Laboratory, Champaign, IL 61824-9005, U.S.A.

(*Received* 11 *August* 1992 *and in final form* 5 *March* 1993)

Abstract—A numerical model was developed to simulate the turbulent mixing processes that occur when a cold fluid flows into a two dimensional tank containing a warmer fluid. The process simulates the charging of a chilled water thermal energy storage tank. The numerical model employs a transient stream function–vorticity formulation to predict the streamline and temperature distributions in the tank. The turbulent effect was modeled by a two equation turbulent model using the turbulent kinetic energy and turbulent length scale equations. The results for a lower corner inlet flow show that the cold fluid will not extensively mix with the warmer fluid in the tank for Archimedean number greater than five and inlet Reynolds number less than 1000. The warm and cold fluids will thermally stratify under these conditions and limitations.

INTRODUCTION

STRATIFICATION of two different temperature fluids is an important consideration in the design of thermal storage tanks. One application is where chilled water flows into the bottom of a storage tank of initially higher temperature or hot water flows in the top of a tank of initially lower temperature. In order to use chilled water in a tank for cool thermal energy storage, the inlet flow must not mix with the warmer fluid in order to form a thermocline in the tank where cold water and hot water are separated by a small region containing the temperature gradient between the cold and warm fluids. This study concerns a cold fluid flowing into a tank of warmer fluid through a horizontal slot located in a bottom corner of the tank.

Matsudaira and Tanaka [1] proposed a model that divided the tank into two regions: a complete mixing region and a piston flow region. In this model, the hot and cold fluids mixed at a certain point, beyond which the flow is uniform and moving parallel to the vertical walls of tank (piston flow). Their model concentrated on the output response of the storage tank without relating it to input conditions.

Oppel *et al.* [2] suggested a one-dimensional model in which turbulent mixing in a tank was simulated by thermal eddy conductivity factors which varied along the depth of an upright cylindrical tank and were determined from experimental data.

Wildin and Truman [3] investigated experimentally a stratified chilled water storage tank. Their scale model experimental results indicated that a nearly one dimensional thermocline will form a Reynolds number less than 800 and a densimetric Froude number less than 1.

Yoo *et al.* [4] investigated experimentally the initial formation of the thermocline and their results suggested that the inlet Froude number is the governing parameter to insure stratification. Abu-Hamdan *et al.* [5] also experimentally studied stratification using variable inlet conditions. They found little effect of the variable inlet temperature conditions over that of conventional inlets.

Nakahara *et al.* [6] investigated thermal storage tanks designs based upon experimental data and proposed a temperature distribution that was assumed one dimensional and combined the piston flow concept with complete mixing flow in the storage tank. The parameter used in the temperature correlation given was determined by experiments.

This study was performed to investigate the mixing process that occurs in a plenum or tank for a side, corner inlet at the bottom of the storage tank, with a cold fluid inflow into the tank initially filled with a hot fluid. The model employs a two-dimensional temperature distribution instead of the one-dimensional approach to determine the resultant streamlines and isotherms for different inlet and storage tank dimensions, inlet flow rates, and fluid temperature differences.

NUMERICAL MODEL

The tank is modeled in a two-dimensional, Cartesian coordinate system. The inlet fluid flow is always

NOMENCLATURE

Ar	Archimedean number, $wg(\Delta\rho/\rho_0)/u_0^2$
C_B	source term coefficient for turbulent length scale
C_D	source term coefficient for turbulent kinetic energy
C_S	source term coefficient for turbulent length scale
C_μ	effective viscosity coefficient
g	gravitational constant
k	turbulent kinetic energy
M	vertical tank dimension
t	turbulent length scale
Pr	Prandtl number
Re	Reynolds number, $u_0 w/\nu$
S_ω	source term
t	time
T	temperature
T_0	flow inlet temperature
T_i	initial temperature in tank
ΔT	$T_i - T_0$
u	velocity in x-direction
u_0	centerline velocity of inlet fluid flow
$\bar{u}$	average inflow fluid velocity
v	velocity in y-direction
w	flow inlet width
X	horizontal tank dimension
x	horizontal direction
y	vertical direction.

Greek symbols

α	thermal diffusivity
β	coefficient of thermal expansion, $-0.05/T_0$
θ	dimensionless temperature, $(T-T_0)/(T_i-T_0)$
μ	dynamic viscosity
ν	kinematic viscosity
ρ	density
$\Delta\rho$	$\rho_i - \rho_0$
Ψ	stream function
ω	vorticity.

Subscripts

eff	effective value
i	initial value
t	turbulent
0	inflow value.

Superscript

$\bar{}$	dimensional values.

assumed to be at a lower temperature than the tank fluid, initially at a uniform temperature.

As shown in Fig. 1, an open ended rectangular tank has a height of twenty times the dimension of the inlet fluid opening. The upper part of the tank is modeled as open with a uniform outlet flow. The lower and vertical boundaries are assumed to be adiabatic and impermeable.

The two-dimensional velocities and temperatures are modeled by a system of five nonlinear, coupled partial differential equations, including the transport equations for stream function and vorticity. The Boussinesq approximation for density is used to account for the buoyancy effects due to temperature dependent density. The turbulence effects are accounted for by using the Prandtl–Kolmogorov formulation of the turbulent viscosity, where the turbulent viscosity is assumed to be dependent upon the turbulence kinetic energy and the turbulence length scale. Both the turbulence kinetic energy and turbulence length scale are calculated from their transport equations. The value of the turbulent viscosity varies throughout the flow field as a function of the turbulence level in the flow. The effective viscosity, defined as the sum of the turbulent viscosity and the molecular viscosity, is used in both the vorticity and temperature transport equations to account for the total molecular and turbulent momentum interchange.

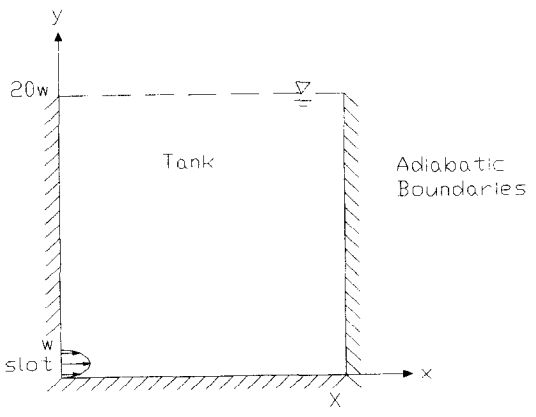

FIG. 1. Schematic of storage tank.

The transport equation for the flow field temperature is derived from the equation for the transport of scalar quantities by a turbulent flow. The effects of flow field turbulence are included by using an effective thermal diffusivity which is defined in terms of the effective viscosity. Since the development of the flow field is of interest in this study, the governing equations are all in transient form.

The equations were normalized using the following parameters:

$$x = \frac{\bar{x}}{M}, \qquad y = \frac{\bar{y}}{M}$$

$$u = \frac{\bar{u}}{u_0}, \qquad v = \frac{\bar{v}}{u_0}$$

$$t = \frac{u_0 \bar{t}}{M}, \qquad \theta = \frac{T - T_0}{T_i - T_0}$$

$$\psi = \frac{\bar{\psi}}{u_0 M}, \qquad \omega = \frac{\bar{\omega} M}{u_0}$$

$$k = \bar{k}/u_0^2, \qquad l = \bar{l}/M.$$

Substituting these terms into the set of governing differential equations results in the following set of nondimensional equations:

Stream function equation:

$$\frac{\partial^2 \psi}{\partial x^2} + \frac{\partial^2 \psi}{\partial y^2} = -\omega. \tag{1}$$

Velocity equation:

$$\frac{\partial \omega}{\partial t} + u\frac{\partial \omega}{\partial x} + v\frac{\partial \omega}{\partial y} = \left[\frac{\partial^2}{\partial x^2}(\mu_{\text{eff}}\omega) + \frac{\partial^2}{\partial y^2}(\mu_{\text{eff}}\omega)\right] \times \frac{1}{u_0 \rho M} + S_\omega, \tag{2}$$

where the source term, S_ω, is

$$S_\omega = 2\left[\frac{\partial^2}{\partial x \partial y}\left(\mu_{\text{eff}}\left(\frac{\partial v}{\partial y} - \frac{\partial u}{\partial x}\right)\right) + \frac{\partial^2}{\partial x^2}\left(\mu_{\text{eff}}\frac{\partial u}{\partial y}\right) - \frac{\partial^2}{\partial y^2}\left(\mu_{\text{eff}}\frac{\partial v}{\partial x}\right)\right]\frac{1}{u_0 \rho M} - \frac{gM}{u_0^2 T_0}\frac{\partial \theta}{\partial x}(T_i - T_0). \tag{2a}$$

The energy equation:

$$\frac{\partial \theta}{\partial t} + u\frac{\partial \theta}{\partial x} + v\frac{\partial \theta}{\partial y} = \left[\frac{\partial}{\partial x}\left(\alpha\frac{\partial \theta}{\partial x}\right) + \frac{\partial}{\partial y}\left(\alpha\frac{\partial \theta}{\partial y}\right)\right]\frac{1}{u_0 M}. \tag{3}$$

The turbulent kinetic energy equation:

$$\frac{\partial k}{\partial t} + u\frac{\partial k}{\partial x} + v\frac{\partial k}{\partial y} = \left[\frac{\partial}{\partial x}\left(\frac{\mu_{\text{eff}}}{Pr_{\text{eff}}}\frac{\partial k}{\partial x}\right) + \frac{\partial}{\partial y}\left(\frac{\mu_{\text{eff}}}{Pr_{\text{eff}}}\frac{\partial k}{\partial y}\right)\right]\frac{1}{\rho u_0 M} + \mu_t\left[2\left(\left(\frac{\partial u}{\partial x}\right)^2 + \left(\frac{\partial v}{\partial y}\right)^2\right) + \left(\frac{\partial u}{\partial y} + \frac{\partial v}{\partial x}\right)^2\right]\frac{1}{\rho M u_0} - C_D\frac{k^{3/2}}{l} + \frac{g\mu_t}{\rho T_0 Pr_t^3}\frac{\partial \theta}{\partial y}(T_i - T_0). \tag{4}$$

The nondimensional turbulent length scale equation:

$$\frac{\partial l}{\partial t} + u\frac{\partial l}{\partial x} + v\frac{\partial l}{\partial y} = \left[\frac{\partial}{\partial x}\left(\frac{\mu_{\text{eff}}}{Pr_{\text{eff}}}\frac{\partial l}{\partial x}\right) + \frac{\partial}{\partial y}\left(\frac{\mu_{\text{eff}}}{Pr_{\text{eff}}}\frac{\partial l}{\partial y}\right)\right]\frac{1}{\rho u_0 M} - C_B\frac{l\mu_t}{k}\left[2\left(\left(\frac{\partial u}{\partial x}\right)^2 + \left(\frac{\partial v}{\partial y}\right)^2\right) + \left(\frac{\partial u}{\partial y} + \frac{\partial v}{\partial x}\right)^2\right]\frac{1}{\rho u_0 M} + C_S k^{1/2} + \frac{lg\mu_t}{kT_0 Pr_t}\frac{(T_i - T_0)}{\rho u_0}\frac{\partial \theta}{\partial y}. \tag{5}$$

The effective viscosity, μ_{eff}, density, ρ, and effective Prandtl number, Pr_{eff}, are given as

$$\rho = \rho_0[1 + \beta(T - T_0)] \tag{6}$$

$$\mu_{\text{eff}} = \mu + \mu_t \tag{7}$$

$$\mu_t = C_\mu \rho k^{1/2} l. \tag{8}$$

$$Pr_{\text{eff}} = \frac{\mu_{\text{eff}}}{\dfrac{\mu}{Pr} + \dfrac{\mu_t}{Pr_t}} \tag{9}$$

and values of the coefficients C were chosen as [7],

$$C_\mu = 0.416, \quad C_D = 0.416, \quad C_S = 0.645, \quad C_B = 1.55.$$

The set of five equations (1)–(5) were solved for u, v, θ, ω, and ψ using a finite difference successive substitution method based on the 'tank and tube' algorithm developed by Gosman *et al.* [8]. Details of the derivation of the finite difference equations are given in Cai [9]. The set of equations were subject to the following boundary conditions:

Jet inflow boundary (Dosanjh and Humphrey [10], Stewart *et al.* [7]):

$$u(y) = \frac{\bar{u}}{u_0} = \frac{2(w - y)y}{w^2} \tag{10}$$

$$\Psi = \int_0^w u(y)\,dy \tag{11}$$

$$\omega = -\frac{\partial u(y)}{\partial y} \tag{12}$$

$$k = 0.01 \tag{13}$$

$$\frac{\partial l}{\partial x} = 0 \tag{14}$$

$$\theta = 0. \tag{15}$$

Bottom (horizontal) boundary:

$$\Psi = k = l = \frac{\partial \theta}{\partial y} = 0 \tag{16}$$

$$\omega = -\frac{\partial^2 \Psi}{\partial y^2}. \tag{17}$$

Vertical walls:

$$\Psi = k = l = \frac{\partial \theta}{\partial x} = 0 \tag{18}$$

$$\omega = -\frac{\partial^2 \Psi}{\partial x^2}. \tag{19}$$

Upper (outflow) boundary:

$$\omega = k = l = 0 \tag{20}$$

$$\frac{\partial \Psi}{\partial y} = 0. \tag{21}$$

The upper boundary, outflow boundary conditions are based upon the assumption that the location of the upper boundary is far enough away from the bottom of the tank that the flow passes through the upper boundary in a normal direction. The temperatures at the upper boundary were determined from extrapolation from the flow field to the boundary.

The initial conditions were chosen as:

$$\theta = 1.0 \tag{22}$$

$$\omega = k = l = 0.0 \tag{23}$$

and the initial condition of the stream function was chosen at a linear interpolation between the two vertical walls. Further details are given by Cai [9].

The relevant nondimensional parameters are Archimedean number and Reynolds number defined as

$$Ar = \frac{wg\dfrac{\Delta\rho}{\rho_0}}{u_0^2} \tag{24}$$

and

$$Re = \frac{u_0 w}{\upsilon}. \tag{25}$$

RESULTS AND DISCUSSIONS

The properties of water at T_0 were chosen for the fluid with density of 1000.0 kg m^{-3}, kinematic viscosity of 1×10^{-6} m^2 s^{-1}, and Prandtl number of 12.0.

The time step in the explicit finite difference solution scheme was chosen to be the largest coverging time step. A time step of 0.0001, which corresponds to about 0.01 s in real time, was used most often. The time step depended upon the inflow velocity and the maximum dimension of the plenum.

The size of the numerical mesh was limited by the available computer memory and computation speed. The size of the mesh was chosen as the minimum number of nodes that assured convergence, determined as a 41 by 81 uniform mesh. Convergence was defined as when the change in ψ and θ from the previous to the present time step was less than 10^{-6}.

The numerical simulations included different tank sizes, fluid inlet widths, inflow velocities, inlet fluid temperatures, and initial tank fluid temperatures. To model a period of nondimensional time of 1 using the 41 by 81 mesh, the computation time is about 10 h on a 486/33 PC. Due to the limitations of available computation speed, most of the simulations were stopped at the dimensionless time of 4. It will be seen, though, that this length of dimensionless time is sufficient to observe the initial mixing of cold and hot fluid in the lower region of the tank.

Table 1. Matrix of parameters

U_0 (m s^{-1})	w (m)	X/w	ΔT (°C)
0.05	0.05	10	0
0.1	0.1	15	5
		20	15

The inlet fluid opening widths of 0.05 m and 0.1 m were used and the velocities ranged between 0.005 to 0.1 m s^{-1}. The difference between initial and inlet temperature ranged from 5 to 15°C. Table 1 is a summary of the different conditions modeled in this study.

For the same tank dimensions and initial temperature difference conditions, four different inflow velocities of 0.005, 0.01, 0.05, and 0.1 m s^{-1} were modeled. The contours of dimensionless isotherms and streamlines are shown in Figs. 2–5 for an inflow Reynolds number of 500. The streamlines shown in Fig. 2 show the cold, higher density fluid entering from the slot and deflects off the right hand wall at $t = 1$. At a dimensionless time of $t = 2$, the flow has deflected off the left hand wall. At $t = 8$, the flow becomes nearly vertical after entering from the corner slot as shown in Fig. 3.

In Fig. 4, the isotherms are much more uniform than expected from the streamline results shown in Figs. 2 and 3. As seen in Fig. 5, the isotherms are nearly parallel at t of 8 even though the thermocline becomes large.

The results for simulations where Ar was greater than 19.6 and Re less than 1000 constitute relatively small banded temperature variation needed for nonmixing and fluid stratification. These results are for the lowest Reynolds numbers and highest Archimedean numbers modeled. The inlet cold fluid remains essentially at the bottom of the plenum and pushes the hot fluid upward. The temperature gradient is almost linear in the vertical direction and nearly zero in the horizontal direction. Under these conditions, it can be assumed that the temperature only varies in the vertical direction.

From the results shown in Figs. 2 through 5, it is seen that for low Reynolds number and high Archimedean number there is no severe mixing. The inflow stream impinges upon the wall opposite to the side jet, changes direction by nearly 180° and impinges again upon the opposite wall above the inlet location. After impinging twice with the walls, the flow finally changes to a direction nearly parallel to the two vertical walls. At this juncture, the major mode of heat transfer between the hot and cold fluids is conduction.

Figures 6 and 7 shows isotherm results for Re of 500 and Ar of 78.4 but for a tank twice as wide as in the previous figures. The isotherm results show that the temperature distribution varies more in the hori-

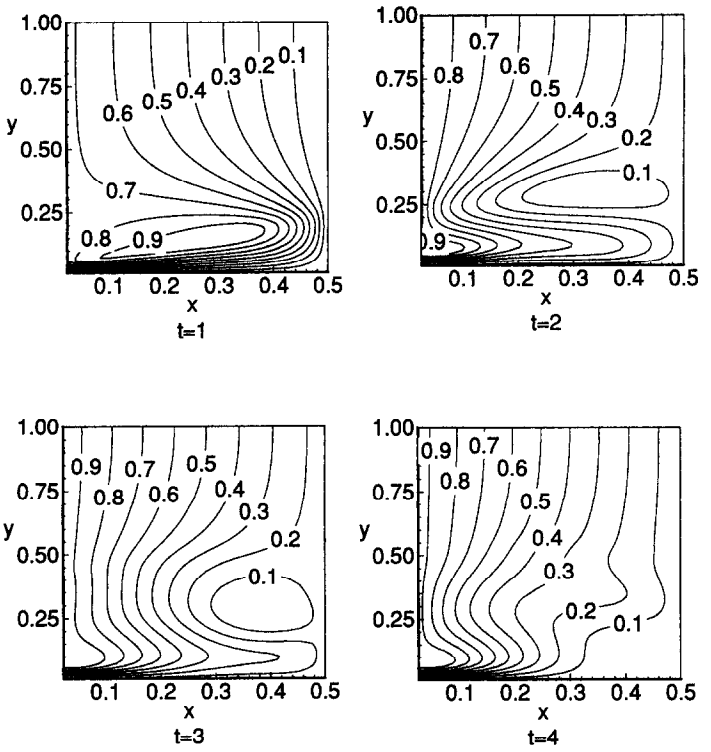

FIG. 2. Streamline results for $Ar = 78.4$, $w/X = 1/10$, $w = 0.1$ m, $\Delta T = 15°C$, $Re = 500$, $t = 1$, 2, 3, and 4.

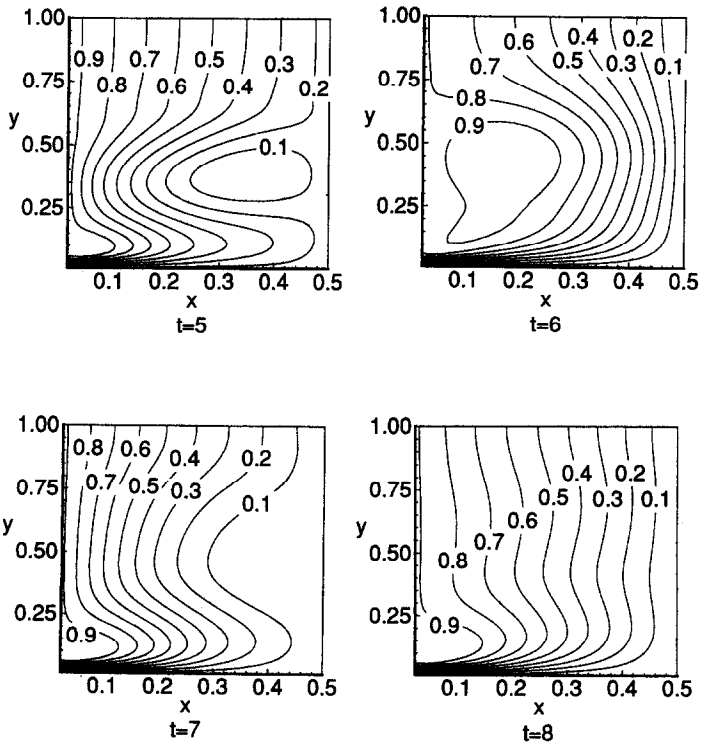

FIG. 3. Streamline results for $Ar = 78.4$, $w/X = 1/10$, $w = 0.1$ m, $\Delta T = 15°C$, $Re = 500$, $t = 5$, 6, 7, and 8.

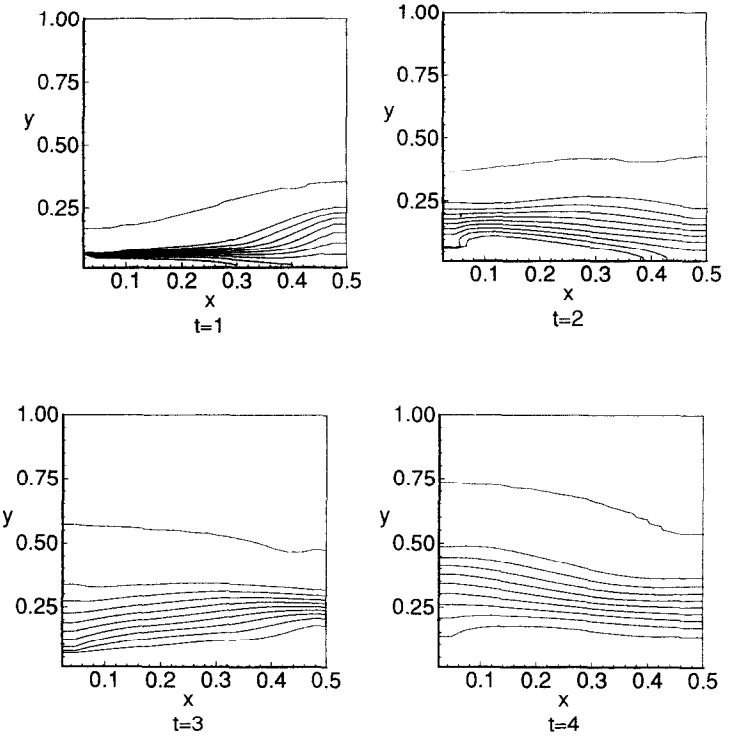

FIG. 4. Isotherm results for $Ar = 78.4$, $w/X = 1/10$, $w = 0.1$ m, $\Delta T = 15^{\circ}$C, $Re = 500$, $t = 1, 2, 3$, and 4.

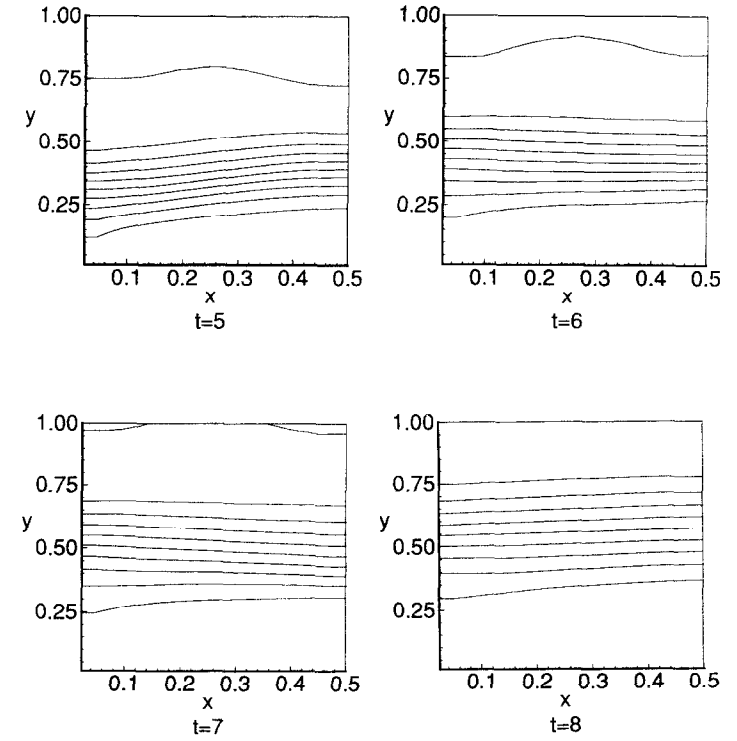

FIG. 5. Isotherm results for $Ar = 78.4$, $w/X = 1/10$, $w = 0.1$ m, $\Delta T = 15^{\circ}$C, $Re = 500$, $t = 5, 6, 7$, and 8.

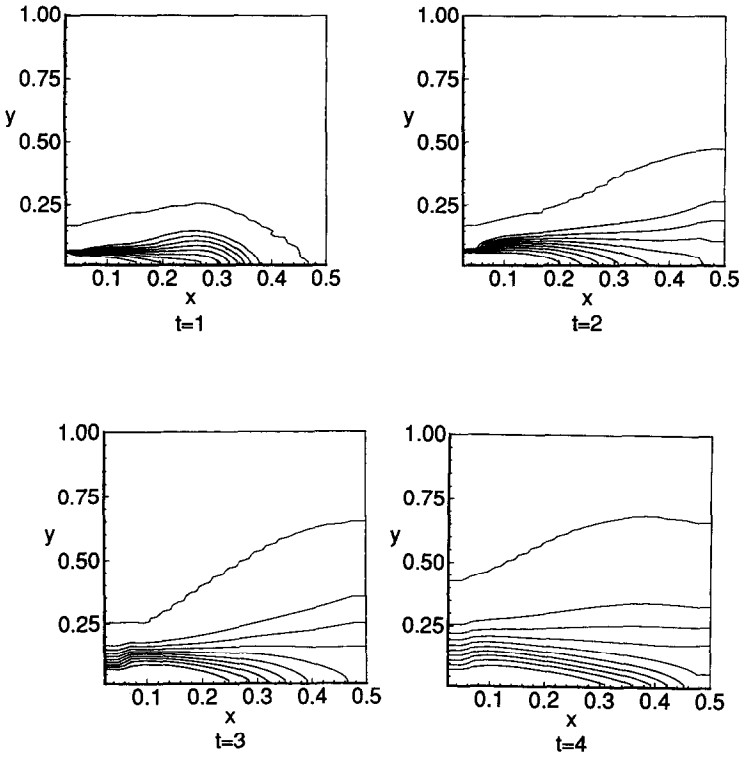

FIG. 6. Isotherm results for $Ar = 78.4$, $w/X = 1/20$, $w = 0.1$ m, $\Delta T = 15°C$, $Re = 500$, $t = 1, 2, 3$, and 4.

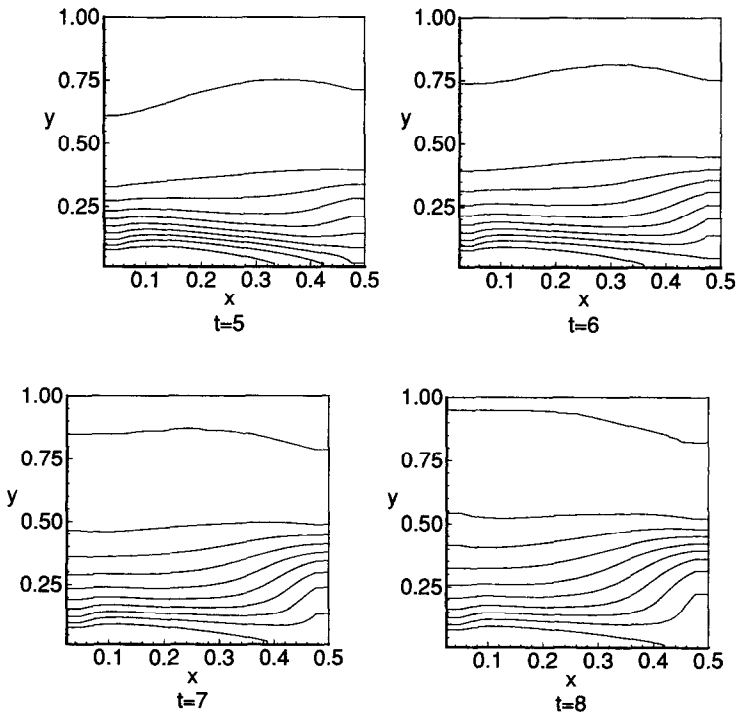

FIG. 7. Isotherm results for $Ar = 78.4$, $w/X = 1/20$, $w = 0.1$ m, $\Delta T = 15°C$, $Re = 500$, $t = 5, 6, 7$, and 8.

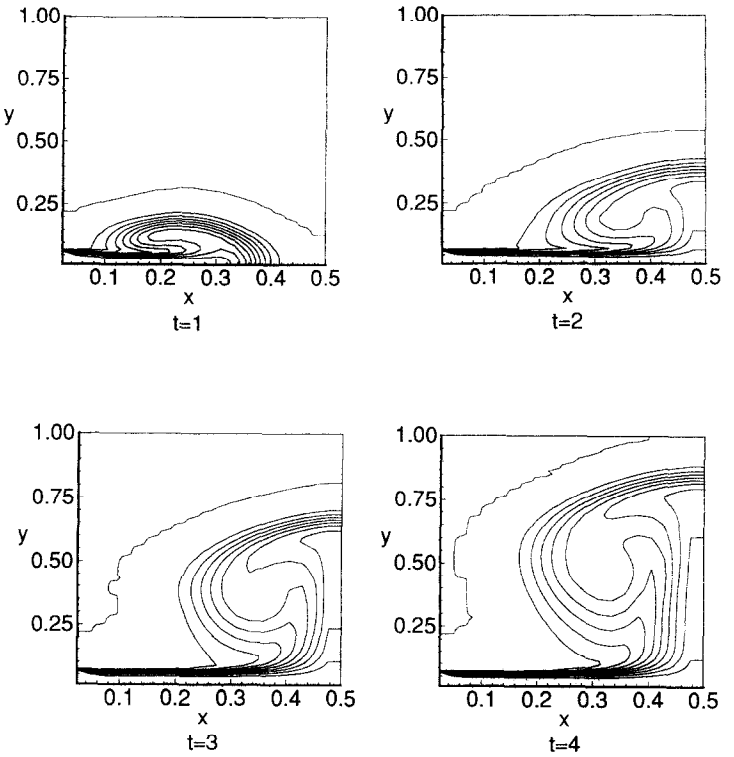

FIG. 8. Isotherm results for $Ar = 0.392$, $w/X = 1/10$, $w = 0.1$ m, $\Delta T = 5$°C, $Re = 5000$, $t = 1, 2, 3$, and 4.

zontal direction, especially in the neighborhood of the two vertical walls, compared to the results in Figs. 4 and 5 for the same Reynolds and Archimedean number. These results show the effect of greater tank width, where the inlet flow loses momentum. When the inlet flow impinges upon the opposite wall, it tends to move up into the tank, causing more mixing. As a result, the temperature distributions near the vertical walls are more distorted. The thermoclines still form but are thicker and more distorted in the horizontal direction. The streamline results, not shown here, reveal that the inlet flow also induces secondary, recirculating flow in the vicinity of the inlet.

Reynolds numbers as high as 10 000 and Archimedean numbers as low as 0.098 were modeled. Both the isotherm and streamline results reveal strong mixing. Because of a much higher initial momentum at the higher Reynolds numbers, as soon as the inflow stream collides with the facing wall, it splits into two streams. One of the streams changes its direction by 90° toward the upper boundary. The other stream moves to the center of the tank and forms an intense vortex. This vortex induces further turbulent mixing and produces an extremely irregular temperature distribution. The temperature gradient develops vertically instead of horizontally. The temperature distribution is multidimensional under these conditions.

The effect of a lower Ar, 0.098, and higher number, 5000, on the isotherms are shown in Figs. 9 and 10, where thermal mixing occurs preventing the formation of a thermocline as was the case in Fig. 5 at a Re of 500. From the isotherm contours results, at low inlet velocities of 0.005 and 0.01 m s^{-1} (Re of 500 and 1000 respectively) isotherms remain nearly parallel to the bottom of the tank. Streamline results show that the inlet cold fluid displaces the warmer fluid toward the top of the tank without severe mixing. At higher inlet velocities (0.05 m s^{-1} and higher), ($Re \geqslant 5000$) both isotherm and streamline results show that there is severe mixing between the cold and hot fluids, as shown in the isotherm results in Fig. 10.

For the highest inlet fluid velocity (0.1 m s^{-1}), under all the geometry and temperature conditions modeled, the results show even more mixing. With Reynolds numbers on the order of 10 000 and the Archimedean number on the order of 0.1, the flow leaves at a high momentum and impinges on the opposite wall, developing a large vortex. Isotherms are irregular and turbulent mixing occurs in the entire tank. Typical results can be seen in Figs. 10 and 11 for Re of 5000 and Ar of 0.098 for streamlines and isotherms, respectively, for $t = 1$ to 4. When the inflow velocity is relatively high, it will take more time and distance for the density gradient to overcome the higher initial momentum.

The effects of initial temperature differences between the inflow and tank fluids show that the temperature differences have a strong affect upon the flow field. Greater temperature differences yield larger density gradients, allowing the inflow cold fluid to more easily stay at the bottom of the tank. This is apparent from comparing Fig. 2 at $t = 2$ with Fig. 11, where the temperature difference is 15°C and 0°C,

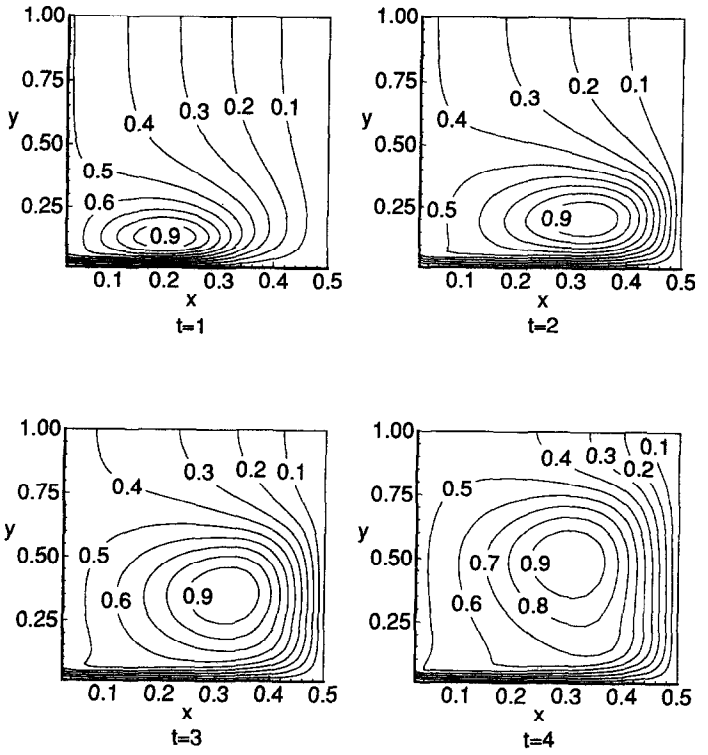

FIG. 9. Streamline results for $Ar = 0.098$, $w/X = 1/10$, $w = 0.1$ m, $\Delta T = 15°C$, $Re = 5000$, $t = 1$, 2, 3, and 4.

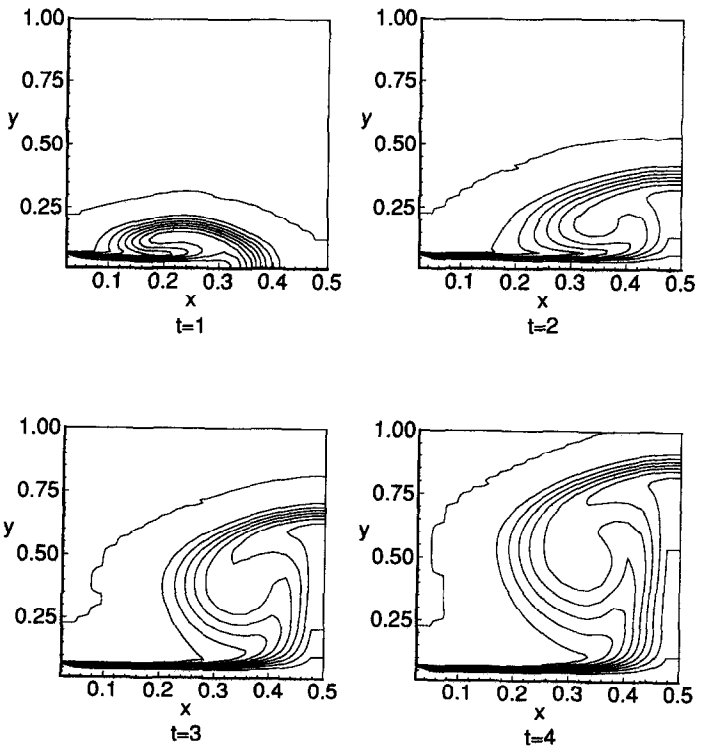

FIG. 10. Isotherm results for $Ar = 0.098$, $w/X = 1/10$, $w = 0.05$ m, $\Delta T = 15°C$, $Re = 5000$, $t = 1$, 2, 3, and 4.

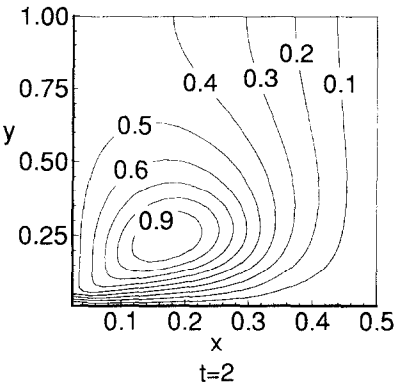

FIG. 11. Streamline results showing the effect of zero initial fluid temperature difference for $t = 2$, $\Delta T = 0$°C, $x/W = 1.10$, $w = 0.1$ m, $Re = 500$, $Ar = 0$.

respectively. When there is no density gradient as in Fig. 11, the inflow stream changes its direction becoming parallel to the opposite wall even at the lower Reynolds number of 500. When there exists a density gradient, as in Fig. 2, the inflow stream tends to stay at the bottom of the tank.

CONCLUSIONS

Flow of cold fluids from a lower corner inlet into a large storage tank containing a higher temperature fluid were investigated to determine the conditions when the fluids would remain nearly thermally separated, or stratified. Stratification of the corner inlet flow is dependent upon inlet Archimedean and Reynolds numbers. Values of Archimedean number greater than 5 and Reynolds number smaller than 1000 provide for vertical stratification between the warm and cold fluids and for nearly zero gradients in the horizontal direction of the tank. The buoyancy force due to the different inlet and initial tank fluid temperature differences has a strong effect on the formation of near zero horizontal temperature gradients. The larger the temperature differences (Archimedean number) between the inflow fluid and the tank fluid, the more easily the horizontally zero gradients and the large cold/hot fluid vertical temperature gradients are formed.

The size of the tank relative to the inlet size has an effect upon the resultant temperature distribution. The larger the ratio of the size of the tank to the size of the inlet, the larger is the increase in the thickness of the vertical temperature gradient between the cold and hot fluids. The depth of the gradient is first determined by the initial mixing and subsequently increases due to conduction heat transfer between the cold and hot fluids.

REFERENCES

1. H. Matsudaira and Y. Tanaka, Dynamic characteristics of a heat storage water tank. Part I, *ASHRAE Transactions* **86**(1), 110–124 (1979).
2. F. J. Oppel, A. J. Ghajar and P. M. Moretti, A numerical and experimental study of stratified thermal storage, *ASHRAE* **92**(2A), 293–309 (1986).
3. M. W. Wildin and C. R. Truman, Evaluation of stratified chilled-water storage techniques, EM-4352, Electric Power Research Institute Vols. 1 and 2 (1985).
4. J. Yoo, M. W. Wildin and C. R. Truman, Initial formation of a thermocline in stratified thermal storage tanks, *ASHRAE Transactions* **92**(2A), 280–291 (1986).
5. M. G. Abu-Hamben, Y. H. Zurigat and A. J. Ghajar, An experimental study of a stratified thermal storage under variable inlet temperature for different inlet designs, *Int. J. Heat Mass Transfer* **35**, 1927–1934 (1992).
6. N. Nakahara, K. Sagara and M. Tsujimoto, Water thermal storage tank: Part 2—mixing model and storage estimation for temperature stratified tanks, *ASHRAE Transactions* **95**(2), 371–394 (1989).
7. W. E. Stewart, Jr., B. R. Becker, L. Cai and C. W. Sohn, Downward impinging flows for stratified chilled water storage, *Proceedings of the 1992 National Heat Transfer Conference*, HTD-Vol. 206-2, pp. 131–138, American Society of Mechanical Engineers (1992).
8. A. D. Gosman, W. M. Pun, A. K. Runchal, D. B. Spalding and M. Wolfshtein, *Heat and Mass Transfer in Recirculating Flows*. Academic Press, London (1969).
9. L. Cai, Turbulent buoyant flows into a two dimensional plenum, M.S. Thesis, University of Missouri, Columbia, MO (1992).
10. S. Dosanjh and J. A. C. Humphrey, The influence of turbulence on erosion by a particle-laden fluid jet, *Wear* **102**, 309–330 (1985).